Biosensors and Bioelectronics 79 (2016) 294–299

Contents lists available at ScienceDirect

Biosensors and Bioelectronics

journal homepage: www.elsevier.com/locate/bios

Designing anthraquinone–pyrrole redox intercalating probes for electrochemical gene detection

Yu-Jen Lin [a], Yung-Chao Wu [b], Veerappan Mani [a,b], Sheng-Tung Huang [a,b,*], Chih-Hung Huang [b], Yi-Chiuen Hu [c], His-Chi Peter Shan [d]

[a] Department of Chemical Engineering and Biotechnology, National Taipei University of Technology, Taipei, Taiwan, ROC
[b] Graduate Institute of Biomedical and Biochemical Engineering, National Taipei University of Technology, Taipei, Taiwan, ROC
[c] National Applied Research Lab, Hsinchu, Taiwan, ROC
[d] WinSense Biotech Corporation, Hsinchu, Taiwan, ROC

ARTICLE INFO

Article history:
Received 1 October 2015
Received in revised form
30 November 2015
Accepted 15 December 2015
Available online 17 December 2015

Keywords:
DNA sensor
Polymerase chain reaction
Electrochemistry
Biosensor
DNA amplification
Molecular design

ABSTRACT

The real-time quantitative electrochemical monitoring of nucleic acid amplification through PCR is a promising renowned methodology to detect pathogenic DNAs. In this work, anthraquinone–pyrrole derivatives based redox intercalating probes (AP probes: AP1, AP2) have been designed, synthesized, characterized and successfully demonstrated in real-time like quantitative PCR. The rationally designed AP probes exhibited excellent DNA binding abilities and electrochemical behaviors. The binding parameters such as binding constant, binding site size and diffusion coefficient were estimated which were comparable to literature reports. Besides, the AP probes are highly stable under PCR thermal conditions and did not inhibit PCR. Therefore, a real-time like quantification of DNA amplification was demonstrated to quantify the initial copy number of target genes. The probe AP2 has excellent ability to detect $\sim 10^3$ copies of target *tpc* DNA with good sensitivity. The AP probes are metal-free, easily synthesizable, non-toxic, thermally stable and feasible for miniaturized PCR chips.

1. Introduction

The sensitive real-time quantitative gene analysis is extremely important in clinical diagnostics, food safety testing and environmental monitoring (Hsieh et al., 2015). The point-of-care use in clinical diagnostics requires simple and portable devices for rapid monitoring of pathogenic genes directly from untreated samples. In this regard, real-time polymerase chain reaction (PCR) amplification strategy is the most successful approach attributed to its accurate quantification of initial copy numbers of target DNA (Defever et al., 2011; Won et al., 2011). Current quantitative PCR (qPCR) instruments are based on the optical detection methods incorporated with fluorescent reporters such as intercalating dyes (Gašparič et al., 2010), primer-based chemistries (Nazarenko et al., 2002) and sequence specific oligonucleotides based chemistries (Kutyavin et al., 2000). Despite their significant success, their use is limited in centralized laboratories due to their high cost, tedious nucleic acid modification, and bulky (Higuchi et al., 1992). In recent times, electrochemical methods are likely to be the best alternative to replace laborious optical methods attributed to their additional advantages of low cost, portable and easier to handle. Therefore, current research in this area has been motivated to develop adaptable electrochemical approaches for the gene detections (Defever et al., 2011; Patterson et al., 2013). The first such effort was demonstrated in 2006 by Hsing et al.; within 8 years, numerous approaches have already been developed which were shown comparable performances to optical methods. The electrochemical monitoring of DNA amplification is based on electrochemical changes revealed by the redox reporters associated with amplification process (Yeung et al., 2006). Patterson et al. (2013) classified the electrochemical PCR monitoring methods into four classes; (1) solid-phase PCR amplification with electrode-bound redox reporters (Yeung et al., 2006), (2) solution-phase PCR using intercalating redox reporters (3) solution-phase PCR with redox labeled probes (Luo et al., 2011; Defever et al., 2009) and (4) isothermal amplification method (Nagatani et al., 2011). Among them, the solution-phase PCR coupled with DNA intercalating reporter has great possibility for sensitive DNA analysis due to its principle similarity with DNA-intercalating fluorescent dyes of optical qPCR. Defever et al. (2011) developed osmium based intercalating redox probes to detect human cytomegalovirus DNA; however, the use of Os metal imposed toxicity concern. Won et al., developed methylene blue based redox probe to detect *Chlamydia*

* Corresponding author at: Department of Chemical Engineering and Biotechnology, National Taipei University of Technology, Taipei, Taiwan, ROC.
E-mail address: ws75624@ntut.edu.tw (S.-T. Huang).

http://dx.doi.org/10.1016/j.bios.2015.12.042
0956-5663/

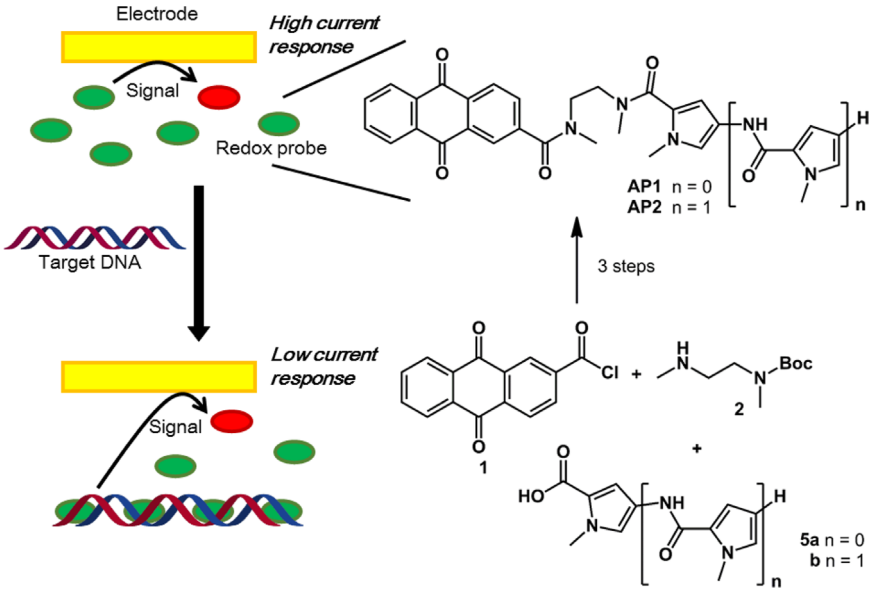

Scheme 1. The schematic representation for syntheses of anthraquinone–pyrrole redox intercalating probes and their application in real-time electrochemical monitoring of DNA amplification.

trachomatis genomic DNA; (Won et al., 2011) however, methylene blue encounters thermal instability in miniaturized PCR chips. Although numerous intercalating redox probes are available for DNA binding (Seio et al., 2005), so far only two intercalating redox probes are exploited in solution-phase PCR.

Anthraquinones are well-known feasible redox system and critically acclaimed for their DNA binding abilities (Wei et al., 2012). Besides, polyamide anchors comprising pyrrole moiety are efficient DNA binding motifs for the recognition of DNA minor groove (Schmidt and Heckel, 2009). Considering the excellent DNA binding attributes of anthraquinone and pyrrole, herein, we have designed anthraquinone–pyrrole (AP1 and AP2) based DNA intercalating redox probes to electrochemically monitor DNA quantification in PCR (Scheme 1 and Scheme S1). Structurally, the probes AP1 and AP2 are equipped with anthraquinone as redox reporter and pyrrole as binding motif through amide linkage. The main objective of this work is to develop anthraquinones–pyrrole based intercalating redox probes for rapid and low-cost gene detection. The probes are thermally stable under PCR conditions without causing PCR inhibition. A real-time like electrochemical monitoring of DNA amplification in PCR was demonstrated which detects $\sim 10^3$ copies of *tpc* plasmid DNA.

2. Experimental

2.1. Reagents and instrumentation

Calf thymus DNA was purchased from Sigma and dissolved in double-distilled water. The concentration of DNA was determined by spectrophotometry at wavelength of 260 nm with molar extinction coefficient of 6600 cm^{-1}. The stock solutions were prepared using double-distilled water and stored at 4 °C. DNA ladder (100–10000 bp), primer TPC-F (CAGGCGCGGATCTCCAG) and primer TPC-R1 (GTCGTCCAGCGCCGTGA) were purchased from Genomics. Plasmid miniPREP bought from GeneDireX was employed for the purification of *tpc* plasmid. Taq. DNA polymerase kits bought from NovelGene was used for the PCR amplification analyses. All the other chemicals were purchased from Sigma-Aldrich, Alfa Aesar and Wako.

N,N-dimethyl-9,10-dioxo-9,10-dihydroanthracene-2-carboxamide (AQ-amide) was prepared by known procedure (Degrand and Miller, 1981) and characterized by ^{1}H NMR, ^{13}C NMR and Mass spectroscopy. The reactions which require anhydrous conditions were performed in oven-dried glassware under an Ar or N_2 atmosphere. Chemicals and solvents were either puriss p.a. or purified by standard techniques. Analytical thin-layer chromatography (TLC) was performed on a glass plate-mounted silica gel $60F_{254}$ (Merck) (0.2 mm thickness). Flash column chromatography was performed using Silicycle silica gel 60. The synthesized compounds were characterized using ^{1}H NMR (Bruker Advance 300 MHz) and ^{13}C NMR (Bruker Advance 75 MHz). Mass spectra were recorded using Finnigan TSQ 700 triple quadrupole mass spectrometer equipped with an electrospray ionization (ESI) ion source. The UV–vis spectroscopy and Fourier-transform infrared spectroscopy analyses were carried out using JASCO V-630, and HORIBA 720, respectively. The Biometra TPersonal Thermocycler was employed for thermal cycling process. Circular dichroism (CD) spectroscopy was performed using Jasco J-810 Spectropolarimeter. Electrochemical measurements were carried out using CHI 612D electrochemical work station. Electrochemical studies were performed in conventional three electrode cell using gold electrode as a working electrode (2 mm diameter), Ag|AgCl (saturated KCl) as a reference electrode and Pt wire as a counter electrode. Prior to use, the working electrode was polished with 0.05 μm alumina powder and thoroughly washed with double distilled water. Prior to each electrochemical experiment, the electrolyte solutions were deoxygenated with pre-purified nitrogen for 5 min unless otherwise specified. All the electrochemical experiments were carried out at room temperature (20 °C). Differential pulse voltammetry (DPV) parameters: amplitude 0.05 V, pulse width 0.05 s and pulse period 0.5 s. The PCR amplification *tpc* (220 bp) sequence conditions were optimized using gel electrophoresis. The PCR products were electrophoresed using agarose gel and visualized by ethidium bromide staining.

2.2. Synthesis of AP1 and AP2

2.2.1. Synthesis of tert-butyl methyl(2-(N-methyl-9,10-dioxo-9,10-dihydroanthracene-2-carboxamido)ethyl)carbamate (**3**)

Anthraquinone-2-carbonyl chloride (**1**, 0.91 g, 3.4 mmol) was dissolved in dry dichloromethane (20 mL), subsequently [2-

(methylamino) ethyl] carbamate (**2**, 0.98 g, 5.23 mmol) and dry triethylamine (14 mL) were added to the solution. Next, the reaction mixture was stirred for 4 h at room temperature. The reaction mixture was added with water and extracted with EA (2 × 50 mL); the organic layer was dried over anhydrous $MgSO_4$, and the solvent was evaporated to get crude product. The crude product was purified by silica gel column chromatography eluting with hexane/ethyl acetate, 3:1 v/v, to gain yellow oil **3** (1.41 g, 98%). ^{1}H NMR (300 MHz, $CDCl_3$): δ=1.44(t, 9H), 2.94(t, 3H, J=4.9 Hz), 3.15(t, 3H, J=2.2 Hz), 3.54(d, 2H), 3.72(d, 2H), 7.78(s, 3H), 8.29(m, 4H).

*2.2.2. N-methyl-N-(2-(methylamino)ethyl)-9,10-dioxo-9,10-dihydroanthracene-2-carboxamide TFA salt (**4**)*

The anthraquinone derivative **3** (2.3 mmol) was dissolved in 50% of TFA in CH_2Cl_2 (v/v) under Ar atmosphere at room temperature. After being stirred for 2 h, the reaction mixture was concentrated *in vacuo*. The obtained crude residue was used in the next step without further purification.

2.2.3. Synthesis of N,1-dimethyl-N-(2-(N-methyl-9,10-dioxo-9,10-dihydroanthracene-2-carboxamido)ethyl)-1H-pyrrole-2-carboxamide (AP1)

1-methylpyrrole-2-carboxylic acid (**5a**, 0.194 g, 1.55 mmol), HATU (0.707 g, 1.86 mmol) and dry triethylamine (0.7 mL, 4.65 mmol) were dissolved in dry DMF (6 mL). The mixture was stirred for 5 min at room temperature. Subsequently, the crude **4** (1.23 mmol) was added to this solution with stirring (Suzuki et al., 2005). Stirring was continued at room temperature for overnight. At the end of this period, the reaction mixture was extracted with EA (3 × 50 mL). The combined organic layers were washed with brine (3 × 50 mL), and were finally dried over $MgSO_4$. This was evaporated to obtain a yellow oil product and the crude product was purified by silica gel column chromatography eluting with hexane/ethyl acetate, 3:1 v/v, to gain white solid AP1 (0.412 g, 78%). ^{1}H NMR (300 MHz; $CDCl_3$, ppm): δ=2.98(t, 4 H, J=28.2 Hz), 3.29(s, 3 H), 3.75(s, 3 H), 3.82(s, 3 H), 5.97(t, 1 H, J=2.9), 6.39(d, 1 H, J=2.4 Hz), 6.61(d, 1 H, J=16.5), 7.70(m, 3 H), 8.19(s, 4 H) ppm. ^{13}C NMR (300 MHz; $CDCl_3$, ppm): δ=33.43, 35.77, 37.57, 44.65, 48.59, 106.74, 113.73, 124.09, 124.70, 125.30, 126.41, 127.09, 127.40, 127.68, 132.31, 133.08, 133.24, 133.44, 134.13, 141.67, 164.22, 169.53, 182.08, 182.21. **ESI-MS** (ESI+): Calcd for $C_{25}H_{23}N_3O_4$= 429.17, found (m/z)= 430.2 $[M+H]^+$.

2.2.4. Synthesis of N,1-dimethyl-4-(1-methyl-1H-pyrrole-2-carboxamido)-N-(2-(N-methyl-9,10-dioxo-9,10-dihydroanthracene-2-carboxamido)ethyl)-1H-pyrrole-2-carboxamide (AP2)

The acid **5b** (0.872 g, 3.53 mmol), HATU (1.61 g, 4.24 mmol) and dry triethylamine (1.5 mL, 10.6 mmol) were dissolved in dry DMF (13 mL) (Thomas et al., 2002). The mixture was stirred for 5 min at room temperature. Subsequently, the crude **4** (4.24 mmol) was added to this solution with constant stirring for overnight at room temperature (Suzuki et al., 2005). At the end of this period, the reaction mixture was extracted with EA (3 × 50 mL). The combined organic layers were washed with brine (3 × 50 mL), and were finally dried over $MgSO_4$. This was evaporated to obtain a yellow oil product. The crude product was purified by silica gel column chromatography eluting with hexane/ethyl acetate, 3:1 v/v, to gain red solid AP2 (1.40 g, 72%). ^{1}H NMR (300 MHz; $CDCl_3$, ppm): δ=2.97(t, 3H, J=34.5 Hz), 3.29(s, 3H), 3.73(s, 3H), 3.84(s, 3H), 3.91(s, 3H), 6.01(t, 1H, J=2.4 Hz) 6.35(d, 1H, J=2.3 Hz), 6.68 (m, 2H), 7.65(d, 1H, J=7.8 Hz), 7.74(m, 3H), 8.23(m, 4H) ppm. ^{13}C NMR (300 MHz; $CDCl_3$, ppm): δ=29.30, 35.50, 36.37, 37.17, 44.24, 105.05, 106.88, 111.70, 117.57, 120.98, 122.13, 125.16, 126.97, 127.25, 131.76, 132.89, 132.93, 133.10, 133.28, 133.94, 133.99, 141.30, 158.94, 163.76, 169.52, 181.97, 182.08 ppm. ESI-MS (ESI+): Calcd for $C_{31}H_{29}N_5O_5$ 551.22, found (m/z)=552.1 $[M+H]^+$.

2.3. Experimental conditions for PCR

In order to employ AP1 and AP2 in real-time like quantitative PCR analyses, all the experiments were carried out under PCR conditions. 1X PCR buffer was used for all experiments which was prepared by following reagents: 15 mM Tris–HCl (pH=8.75), 50 mM KCl, 2 mM $MgCl_2$, 0.1% Triton X-100 and 1% DMSO. The real-time like electrochemical PCR analyses of *tpc* DNA (220 bp) were carried out in 1X PCR buffer containing 0.25 mM dNTP, 0.25 μM of each forward (Primer-R1) and reverse (Primer-F) primers, 1.25 units Taq. DNA polymerase, *tpc* plasmid DNA and DMSO. The volumes and concentrations of each components used for the PCR analyses were given in Table S1. The PCR analyses were carried out in accordance with the following thermal cycling conditions (total of 40 cycles): preheating period of 5 min at 95 °C, followed by denaturation for 30 s at 94 °C, annealing at 55.2 °C for 20 s and elongation period of 1 min at 72 °C.

3. Results and discussions

A detailed scheme for the syntheses of AP1 and AP2 are outlined in Scheme S2. The AP1 and AP2 were prepared from three precursors, anthraqunine-2-carbonyl chloride (**1**), mono Boc protected diamine (**2**) and pyrolic acid **5a–b**. Synthesis of AP1 to AP2 was completed in three steps, giving an overall yield of 70-76% from (**1**). The chemical structures of the synthetic intermediates and final products were characterized by NMR, and mass spectroscopy, and the results are listed in the experimental section.

3.1. Electrochemical and optical properties of the probes

The electrochemical behavior of AP1 (curve a, Fig. 1A), AP2 (curve a, Fig. 1B) and AQ-amide (curve a, Fig. 1C) were investigated by cyclic voltammetry. The potential range was applied between –0.3 V and –0.8 V, while the scan rate was held at 50 mV s^{-1}. Both AP1 and AP2 exhibits characteristic quasi-reversible redox peaks of quinone–hydroquinone redox couple which involves two electrons and two protons (Scheme S3). The important electrochemical parameters such as anodic peak potential (E_{pa}) and cathodic peak potential (E_{pc}), anodic peak current (I_{pa}) and cathodic peak current (I_{pc}), peak potential (E_p), half-wave potential ($E_{1/2}$) and I_{pa}/I_{pc} ration were evaluated and given as Table S2. Both AP1 and AP2 exhibit similar redox potential values, while the peak currents have marginal variation which might be due to the differences in number of linked pyrrole moieties (Valencia and González, 2011). UV–visible spectra have been carried out in order to understand optical properties of the probes. The spectra of AP1 and AP2 exhibited the fundamental absorption peak of anthraquinone located around 260 nm which is consistent with literature values (Spruit, 1949). The values of absorbance and molar absorptivity (ϵ) were given in Table S3.

3.2. DNA intercalating abilities of AP1 and AP2

Fig. 1 shows the cyclic voltammograms obtained for AP1 (A) and AP2 (B) and AQ-amide (C) in absence (a) and presence of 200 μM calf thymus DNA. In presence of DNA, the peak currents of anthraquinone redox couple are significantly reduced which indicates good DNA binding nature of AP1 and AP2. Possibly, the planar structure of anthraquinone was efficiently embedded and intercalated by DNA double helix with the help of pyrrole moiety. In addition, the usually associated week interactions such as van der Waals, hydrogen bonding and π–π stacking interactions were also contributed in binding. The control sample, AQ-amide is unable to bind with DNA which is evident from the observation of

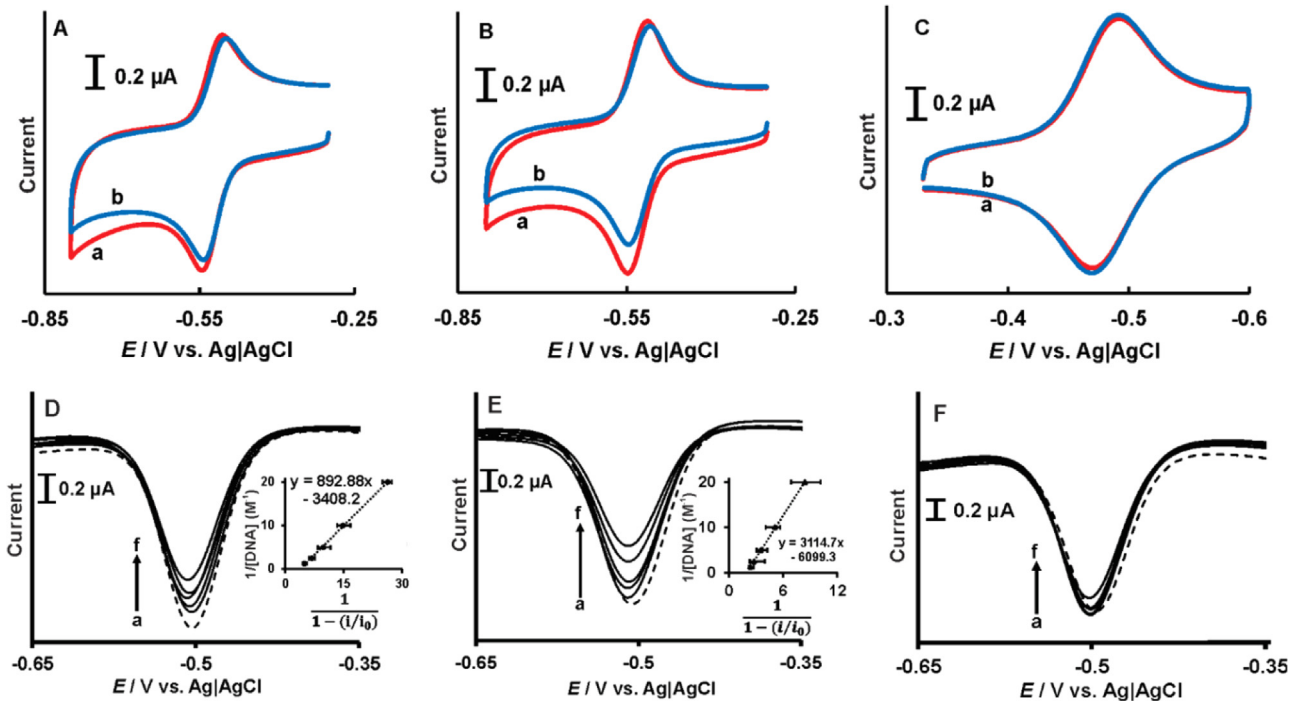

Fig. 1. Cyclic voltammograms obtained for 40 μM AP1 (A), AP2 (B) and AQ-amide (C) in absence (a) and presence (b) of 200 μM calf thymus DNA under experimental condition. DPVs obtained for 40 μM AP1 (D), AP2 (E) and AQ-amide (F) in absence (a) and presence of 50 μM (b), 100 μM (c), 200 μM (d), 400 μM (e) and 800 μM (f) calf thymus DNA under experimental condition. Inset: Plot of 1/[DNA] vs. $1/(1–i/i_0)$.

same redox peak currents in presence and absence of DNA (Fig. 1C). These results indicating that the specially designed pyrrole moieties (binding motifs) embedded in probes (AP1 and AP2) play an important role in DNA binding process. Also, the number of pyrrole moieties has significant influence on DNA binding. Fig. S1 shows the CD spectra recorded for fixed concentration of calf thymus DNA (100 μM) in absence and presence of AP1 (A), AP2 (B), and AQ-amide (C). The increasing concentrations of AP1 and AP2 caused significant changes in optical rotation number, while induced CD signals were observed at 280 nm which are strong evidences for the DNA-probe interaction. The induced CD signals are due to the formation of DNA-probe complex which occurred through interaction between transition moments of probes and chirally disposed surroundings of DNA base (Zhong et al., 2004). However, AQ-amide did not show any obvious changes indicating its impotence to intercalate with DNA.

3.3. Binding constant, binding site size, diffusion co-efficient

Fig. 1 presents the DPVs obtained for AP1 (D), AP2 (E) and AQ-amide (F) in absence (a) and presence of calf thymus DNA under experimental conditions. For each addition of DNA, I_{pc} of anthraquinone redox couple was decreases which are consistent with voltammogram results. The plots between 1/[DNA] and $1/(1–i/i_0)$ for AP1 and AP2 were given as insets to Figs. 1D and E. The following Eq. (1) was used to calculate binding constants (K_b) of probes.

$$\frac{1}{[\mathrm{DNA}]} = \frac{K_b(1-A)}{1-(\frac{i}{i_0})} - K_b \quad (1)$$

where, K_b is binding constant, i and i_0 are peak currents obtained for probes with and without DNA and A is proportionality constant. The values of K_b obtained for AP1 and AP2 are $3.408 \times 10^3\ M^{-1}$ and $6.099 \times 10^3\ M^{-1}$ respectively (Table 1). The value of K_b increased as the number of pyrrole group increases.

Table 1
DNA intercalating parameters estimated for AP1, AP2 and AQ-amide. Here, K_b is binding constant, s is binding site size, D_f is diffusion coefficient of free probes (absence of calf thymus DNA) and D_b is diffusion coefficient of bound probes (in presence of 100 μM of calf thymus DNA). bp = base pairs.

Probes	K_b (M^{-1})	s (bp)	D_f ($cm^2\ s^{-1}$)	D_b ($cm^2\ s^{-1}$)
AP1	3.408×10^3	6	4.521×10^{-12}	4.160×10^{-12}
AP2	6.099×10^3	4	5.842×10^{-12}	4.544×10^{-12}
AQ-amide	–	–	1.043×10^{-11}	1.040×10^{-12}

The K_b values obtained for AP1 and AP2 were comparatively smaller than previous reports (Table S4). Perhaps, the interactions between DNA and AP probes were comparatively weaker than reported probes.

In order to calculate binding site size (s), a plot between C_b/C_f and [DNA] was drawn (Fig. S2), while Eq. (2) was adopted to calculate binding site size (Carter et al., 1989).

$$\frac{C_b}{C_f} = \frac{i-i_0}{i} = \frac{K_b}{2s}[\mathrm{DNA}] - K_b C_b \quad (2)$$

Here, C_b is the concentration of bound probes, C_b is the concentration of free probes, i and i_0 are the peak currents obtained for probes in presence and absence of DNA. K_b is binding constant and s is binding site size per base pair (bp). In literature, the reported s values for DNA intercalated probes are within the size ranges of 1–20 base pairs (Carter et al., 1989). The obtained s values for AP1 and AP2 are 6 and 4 respectively (Table 1), which are in well agreement with the typical ranges reported for the DNA intercalating probes.

The diffusion co-efficient values in absence and presence of DNA were calculated using Randles–Sevcik equation (3),

$$i = 2.69 \times 10^5\ n^{3/2}\ A\ C_0^*\ D^{1/2}\ v^{1/2} \quad (3)$$

Here, n_a is number of electrons involved in the rate-

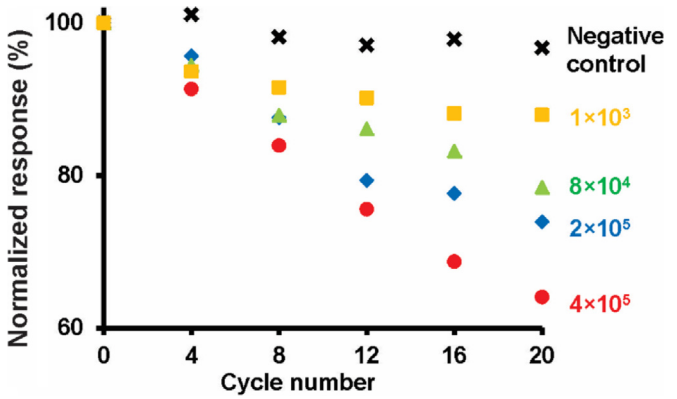

Fig. 2. Plots between normalization peak currents as function of cycle numbers; the negative control (black), 4×10^5 (red), 2×10^5 (blue) and 8×10^4 (green) copies of *tpc* plasmid DNA. (For interpretation of the references to color in this figure legend, the reader is referred to the web version of this article.)

determining step, D ($cm^2\ s^{-1}$) is diffusion coefficient of electroactive species, v is scan rate and C_o^* is concentration of electroactive species. The other terms have their usual meanings. The plot between peak currents and square root of scan rate is given as Fig. S3. The experiments were performed in 40 μM AP1, AP2 and AQ-amide in absence (dotted line) and presence of DNA (solid line) at the scan rates ranging from 0.01 to 0.1 $V\ s^{-1}$ under experimental condition. The diffusion coefficient values in presence and absence of calf thymus DNA were calculated and listed in Table 1. The diffusion co-efficient values of probes were decreased considerably after their intercalation with DNA and this behavior is similar to previous reports. Conversely, AQ-amide is not shown any obvious difference in the diffusion co-efficient values either in presence or in absence of DNA.

3.4. Thermal stability and PCR inhibitory studies

In order to obtain stable electrochemical signals, the probes should be chemically stable under PCR a thermal condition which is one of the important prerequisite for probes. In order to investigate thermal stability, two different concentrations of AP1 and AP2 (30 μM and 50 μM) were prepared in PCR reacting buffer and incubated under optimized PCR conditions for different cycles. Next, DPVs were carried out for each mentioned cycles; stable DPV peak currents as function of cycle numbers were obtained for AP1 and AP2. The calibration plots between number of cycles and response currents of AP1 and AP2 were given as Fig. S4. More than 95% of initial response currents were retained even after 40 thermal cycles which clearly revealed the good thermal stability of AP1 and AP2. Another important requirement for the probes to be used in PCR analysis is that they should not inhibit PCR reactions. The inhibition properties of AP1 and AP2 were investigated by gel electrophoresis at both low (40 μM) and high concentrations (100 μM) of DNA in standard microtubes (Fig. S5). It is worth to mention that strongly binding probes have high potential to inhibit PCR reactions which restricts their application in real-time PCR analysis. As shown in Fig. S5, the PCR reactions were not inhibited in both low and high concentrations of probes. Therefore, AP1 and AP2 are qualified candidates for real-time quantitative electrochemical PCR analysis to detect DNA.

3.5. Real-time like quantitative monitoring of DNA amplification

To demonstrate real-time like qPCR, we have chosen AP2 since it showed better binding affinity over AP1. The PCR materials and AP2 were incubated under PCR condition for 0, 8, 16, 24, 32, 40 cycles and subsequently, DPVs were carried out at each cycles. The DPV currents were decreased during PCR amplification process from 0 to 40 cycles. However, in the absence of primers, PCR sample with all other reagents shows no changes in peak currents (negative control). The normalized response was calculated and plotted against their corresponding cycle numbers (Fig. 2). As shown in figure, AP2 sensitively detects DNA as low as 10^3 copy number of *tpc* (220 bp) sequences. Although, the detection limit of AP2 probe is higher than the optical TaqMan probes, it is comparable to reported electrochemical redox probes such as methylene blue (10^3 copy number) and Os $(bpy)_2$ $DPPZ^{2+}$ (10^3 copy number). Interestingly, the described AP2 probe holds distinctive advantages over reported probes such as metal-free, high thermal stability, easy and cheaper production protocols. In addition, the reported electrochemical determination platform is simple, rapid, sensitive and selective. Currently, we are developing AP series based portable microchips for the real-time quantitative monitoring of DNA amplification.

4. Conclusions

In summary, we have successfully synthesized novel anthraquinone–pyrrole redox intercalating probes for the quantification of DNA. Both AP1 and AP2 have shown good DNA intercalating ability, wherein their binding abilities in terms of binding constant, binding site size and diffusion coefficient were estimated. The probes are thermally stable under PCR conditions without causing PCR inhibition. A real-time like electrochemical monitoring of DNA amplification in PCR was demonstrated which detects $\sim 10^3$ copies of *tpc* plasmid DNA and the detection limit is comparable to previously reported probes, $Os[(bpy)_2DPPZ]^{2+}$ and methylene blue. The AP probes have additional advantages such as metal-free and miniaturizable opportunities. Therefore, these anthraquinone–pyrrole redox probes have great potential for the development of real-time electrochemical quantitative PCR.

Acknowledgment

This work was supported by the Ministry of Science and Technology, Taiwan (103-2811-M-027-002, 102-2113-M-027-002-MY3, 104-2622-M-027-001-CC3, 104-2622-M027-001-CC3).

Appendix A. Supplementary material

Supplementary data associated with this article can be found in the online version at doi:10.1016/j.bios.2015.12.042.

References

Carter, M.T., Rodriguez, M., Bard, A.J., 1989. J. Am. Chem. Soc. 111, 8901–8911.
Defever, T., Druet, M., Evrard, D., Marchal, D., Limoges, B., 2011. Anal. Chem. 83, 1815–1821.
Defever, T., Druet, M., Rochelet-Dequaire, M., Joannes, M., Grossiord, C., Limoges, B., Marchal, D., 2009. J. Am. Chem. Soc. 131, 11433–11441.
Degrand, C., Miller, L.L., 1981. J. Electroanal. Chem. Interfacial Electrochem. 117, 267–281.
Gašparič, M.B., Tengs, T., La Paz, J.L., Holst-Jensen, A., Pla, M., Esteve, T., Žel, J., Gruden, K., 2010. Anal. Bioanal. Chem. 396 (6), 2023–2029.
Higuchi, R., Dollinger, G., Walsh, P.S., Griffith, R., 1992. Biotechnology 10, 413–417.
Hsieh, K., Ferguson, B.S., Eisenstein, M., Plaxco, K.W., Soh, H.T., 2015. Acc. Chem. Res. 48, 911–920.
Kutyavin, I.V., Afonina, I.A., Mills, A., Gorn, V.V., Lukhtanov, E.A., Belousov, E.S., Singer, M.J., Walburger, D.K., Lokhov, S.G., Gall, A.A., 2000. Nucleic Acids Res. 28, 655–661.
Luo, X., Xuan, F., Hsing, I.-M., 2011. Electrochem. Commun. 13, 742–745.
Nagatani, N., Yamanaka, K., Saito, M., Koketsu, R., Sasaki, T., Ikuta, K., Miyahara, T.,

Tamiya, W., 2011. Analyst 136, 5143–5150.
Nazarenko, I., Pires, R., Lowe, B., Obaidy, M., Rashtchian, A., 2002. Nucleic Acids Res. 30, 2089–2195.
Patterson, A.S., Hsieh, K., Soh, H.T., Plaxco, K.W., 2013. Trends Biotechnol. 31, 704–712.
Schmidt, T.L., Heckel, A., 2009. Small 5, 1517–1520.
Seio, K., Mizuta, M., Terada, T., Sekine, M., 2005. J. Organ. Chem. 70, 10311–10322.
Spruit, C., 1949. Recl. Trav. Chim. Pays-Bas. 68, 325–335.
Suzuki, T., Ichioka, K., Higuchi, H., Kawai, H., Fujiwara, K., Ohkita, M., Tsuji, T., Takahashi, Y., 2005. J. Org. Chem. 70, 5592–5598.
Thomas, M., Varshney, U., Bhattacharya, S., 2002. Eur. J. Org. Chem. 2002, 3604–3615.
Valencia, D.P., González, F.J., 2011. Electrochem. Commun. 13, 129–132.
Wei, L., Shao, Y., Zhou, M., Hu, H.-W., Lu, G.-Y., 2012. Org. Biomol. Chem. 10, 8484–8492.
Won, B.Y., Shin, S., Baek, S., Jung, Y.L., Li, T., Shin, S.C., Cho, D.-Y., Lee, S.B., Park, H.G., 2011. Analyst 136, 1573–1579.
Yeung, S.S., Lee, T.M., Hsing, I.-M., 2006. J. Am. Chem. Soc. 128, 13374–13375.
Zhong, W., Yu, J.-S., Liang, Y., Fan, K., Lai, L., 2004. Spectrochim. Acta Part A 60, 2985–2992.